Journal of Ceramic Processing Research. Vol. 18, No. 2, pp. 146~150 (2017)

J O U R N A L O F
Ceramic
Processing Research

Structural and dielectric properties of $CaTiO_3$ synthesized utilizing Duck's eggshell as a calcium source

Akhiruddin Maddu*, Linda Permatasari and Ardian Arif
Biophysics Division, Department of Physics, Bogor Agricultural University, Dramaga Campus, Bogor 16680, Indonesia

$CaTiO_3$ has been synthesized utilizing duck's eggshell waste as calcium source via hydrothermal route followed by heat treatment (sintering). Based on the results of X-ray diffraction analysis was found that the crystalline phase of $CaTiO_3$ highly dependent on the sintering temperature, the higher the sintering temperature resulted in the $CaTiO_3$ phase was increasingly dominant in the sample. Meanwhile, the average crystallite size (ACS) of $CaTiO_3$ increases with the sintering temperature. The results of microstructural observation by scanning electron microscope (SEM) shows the morphology of $CaTiO_3$ was highly influenced by the sintering temperature, the higher the sintering temperature the greater the particle size $CaTiO_3$. The measurement results of dielectrics properties demonstrate the value of the dielectric constant of $CaTiO_3$ increased significantly with increasing sintering temperature.

Key words: $CaTiO_3$, Dielectrics, Eggshell, Hydrothermal, Sintering.

Introduction

Calcium titanate ($CaTiO_3$) is one of a group of metal titanate compounds with a perovskite structure. $CaTiO_3$ has long been known as a ceramic dielectric with a high dielectric constant, namely 160 and large positive temperature coefficient [1]. $CaTiO_3$ has an important application in microwave communication systems [1, 2]. $CaTiO_3$ also be used as an electronic ceramic material (electroceramics) in particular as ferroelectric materials and dielectric materials in general [3, 4].

Electroceramics based on $CaTiO_3$ has been studied various physical properties by a number of researchers. Physical properties of $CaTiO_3$ that have been studied including electrical properties, especially electrical conductivity [5], while the optical properties were widely studied including the nature of the absorption of UV-Vis and photoluminescence performance [6]. Likewise, much studied their thermoelectric properties [5], optical properties [7], electronic structure and photocatalytic activity [8, 9].

Various methods can be performed to synthesize $CaTiO_3$, including sol-gel [10], precipitation [11], mechano-chemical milling [12, 13], electro-chemical deoxidation [14], mechanical alloying [15] and hydrothermal [7, 16]. Each of these methods has advantages and disadvantages. Hydrothermal is a promising method for the preparation process is short and simple, in addition to the product produced has crystallinity better than the other methods [17]. This study used the hydrothermal method to synthesize $CaTiO_3$ that followed by the heating treatment to improve the crystallinity of the product.

$CaTiO_3$ synthesis can be done by utilization of different sources. Calcium (Ca) source can be taken from various commercial sources such as calcium salts ($CaCl_2$ and $CaNO_3$) [6, 7, 10] or oxides of calcium ($CaCO_3$ and CaO) [2, 4, 12-14]. However, the reagents must be purchased at a price that is not cheap. As an alternative to the synthetic reagents, it can be used bioresource materials as a source of calcium to synthesize $CaTiO_3$. Eggshell and shells are known to have a high calcium content that can be utilized to synthesize functional materials based on calcium compounds. Availability of the shells is very abundant and easy to obtain, even just be an underutilized waste.

This research used the duck's eggshells as a source of calcium to synthesize a functional material of $CaTiO_3$ to be explored its dielectric properties. So far, there has been no report on the use of eggshell as a calcium source to synthesize $CaTiO_3$. By utilizing the starting materials from eggshells waste, the cost for the synthesis of $CaTiO_3$ will be reduced. The use of eggshells as starting material to synthesize $CaTiO_3$ was based on the content of calcium in eggshells and its availability is abundant. The main composition of the eggshell is calcium carbonate ($CaCO_3$) of 94% of the total weight of the whole shell, calcium phosphate (1%), organic materials (4%) and magnesium carbonate (1%) [18]. In this study, $CaTiO_3$ was synthesized by hydrothermal method with the reason the process is simple and can produce good crystallinity of the sample.

*Corresponding author:
Tel : +62-251-8625278
Fax: +62-251-8625728
E-mail: akhiruddin@apps.ipb.ac.id

Experimental Procedures

Synthesis of $CaTiO_3$ was conducted by hydrothermal method utilizing duck's eggshell as a calcium source and commercial TiO_2 powder (Aldrich). Eggshell was calcined at a temperature of 600 °C to obtain white powder. To synthesis of $CaTiO_3$, the powder derived from eggshell and commercial TiO_2 powder with mass ratio 1:1, each 2.2 g, were mixed then ground with mortar for 30 minutes. The mixture was placed into the glass beaker then added 50 mL of distilled water while stirred at a speed of 600 rpm for 30 minutes using a hotplate magnetic stirrer. The mixture was poured into the hydrothermal reactor made of stainless steel equipped with a Teflon beaker. The reactor was placed onto a hot plate and start to a hydrothermal process by heating the reactor at a temperature of 200 °C for 3 hrs. The product of hydrothermal process, a white precipitate was filtered and washed several times with distilled water and then dried. The dry powder was divided by three with the same mass and formed into pellets, then heated in the furnace at different temperatures, respectively 700, 800, and 900 °C for 5 hrs.

XRD characterization was conducted to obtain information both quantitatively and qualitatively on the crystal structure of $CaTiO_3$. Based on the diffraction pattern can be determined the crystal phases and crystallite sizes of $CaTiO_3$ samples. The samples were scanned from 2θ = 15-75° using XRD machine with Cu source which has a wavelength of 0.154 nm.

As for studying the surface morphology of $CaTiO_3$ it was observed by using a scanning electron microscope (SEM) with a secondary electron mode. The SEM images will provide information about the shape, size, and uniformity of particles in samples.

Dielectric properties of the $CaTiO_3$ samples were measured using LCR Meter (Hi-Tester 3522-50, Hioki). Measurements were carried out on samples of $CaTiO_3$ in the pellet form with a thickness of 1.1 mm and a diameter of 1.3 cm. The samples were placed between two copper electrodes on the printed circuit board (PCB). Both electrodes were connected to the terminals of LCR Meter. Capacitance was measured in the frequency range of 20 Hz-2 kHz, from which can be calculated the value of the dielectric constant of $CaTiO_3$ sample.

Results and Discussion

Structural properties of $CaTiO_3$ samples were studied by X-ray diffraction from which can be determined the crystal phase and crystallite size of $CaTiO_3$ samples. Fig. 1 shows an X-ray diffraction pattern for the three $CaTiO_3$ samples with different sintering temperatures, respectively at 700, 800, and 900 °C. The samples were scanned at an angle 2θ of 15-75 °. There were significant differences in the diffraction patterns of each sample

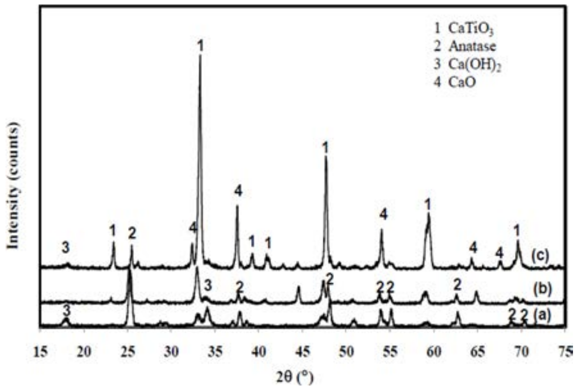

Fig. 1. Difractogram of $CaTiO_3$ sample for sintering at (A) 700 °C, (B) 800 °C, dan (C) 900 °C.

indicating that the sintering temperature affects the structural properties of the samples.

Sample that sintered at a temperature of 700 °C was still dominated by the phases of starting material, mainly TiO_2 anatase. Phases of $Ca(OH)_2$ and CaO also appeared, although not significant when was compared with the phase of TiO_2 anatase. $CaTiO_3$ phase was observed only at 33.18 ° and 47.42 ° with very weak intensity. The sintering temperature of 700 °C was still too low to cause a complete reaction to produce crystalline phase of $CaTiO_3$. Meanwhile, sample which was sintered at 800 °C showed diffraction peaks of $CaTiO_3$ phase with stronger intensity, although not dominating the overall diffraction pattern, as shown in Fig. 1(b). The peaks of $CaTiO_3$ were identified at 32.98 °, 47.46 ° and 59.2 ° representing the presence of crystalline phases of $CaTiO_3$, while the other phases still appears significantly such as starting material TiO_2 anatase and $Ca(OH)_2$ with lower intensity. This means that the sintering temperature of 800 °C has not been able to cause the complete reaction in the formation of pure $CaTiO_3$ compounds.

Further sintering at 900 °C resulted in a very different diffraction pattern. The diffraction pattern has been dominated by the phase of $CaTiO_3$ as indicated by the characteristic peaks with very high intensity when was compared with other peaks, as shown in Fig. 1(c). All of $CaTiO_3$ peaks appeared in diffraction pattern as can be identified at angle (2θ) of 23.4 °, 33.3 °, 47.66 °, 54.42 °, 69.92 ° corresponding to the planes of diffraction (hkl), respectively to (101), (121), (202), (123) and (242). Peaks of (031) and (220) planes also appeared with lower intensity. These peaks were matched with standard XRD data of orthorhombic $CaTiO_3$ (JCPDS card No. 42-0423) [9, 19, 20]. However, there are also significant peaks of CaO phase with strong enough intensity, respectively at around 32 °, 37 °, 54 °, 64 °, and 67 ° [21]. The appearance of CaO phase is predicted due to the release of H_2O molecules from $Ca(OH)_2$ at a higher temperature (900 °C).

Based on the diffraction pattern was found that the

Table 1. Avarage crystallite size of $CaTiO_3$ samples.

Sample	2θ	cos θ	FWHM (rad)	σ (nm)
700°C	25,3413	0,9756	7,656E-3	37,12
800°C	32,9575	0,9589	7,250E-3	39,88
900°C	25,4601	0,9754	6,786E-3	41,89

sintering temperature affects the crystalline phase of the samples. High temperature is a better condition than lower temperatures in the growth of $CaTiO_3$ samples, though sintering at 900 °C was not perfect because there was still another phase that appears, namely CaO with significantly strong intensity. Therefore it is need a higher temperature treatment to produce pure $CaTiO_3$ compound.

Widening the diffraction pattern is influenced by the crystallite size, where the wider diffraction pattern indicates the smaller crystallite size. Average crystal size (ACS) can be calculated based on widening the diffraction peaks using Scherrer formula by the equation below

$$\sigma = 0.9\lambda / B \cdot \cos\theta \qquad (1)$$

where s is the crystallite size (nm), λ is the wavelength of the X-ray source (Cu = 1.59 nm), B is the full-width at half maximum (FWHM) in radians, and θ is half of the diffraction angle. The average crystallite size (ACS) of $CaTiO_3$ samples are summarized in Table 1. The results showed that the average crystallite size (ACS) increased significantly with increasing sintering temperature.

Surface morphology of $CaTiO_3$ samples can be seen in the SEM images taken with a magnification of 30,000 times. Fig. 2 shows the SEM images of the three samples with different sintering temperatures, respectively at 700, 800, and 900 °C. There were differences in the morphology of the three samples, particularly in their particle size and distribution. As can be seen in the SEM images, the higher the sintering temperature the greater the sample particle size of $CaTiO_3$.

$CaTiO_3$ sample which was sintered at a temperature of 700 °C has the size and shape of particles that looks uniform and regular with the grain size smallest than the other samples, the boundaries between the grains can be observed clearly, as shown in Fig. 2(a). While the sample which was sintered at a temperature of 800 °C has a grain that is more diverse both size and shape, and even tend to be irregular, this is due to increase temperature sintering. Inter-granular diffusion mechanism began to occur so that the particles become denser and compact, as shown in Fig. 2(b). Effect of sintering temperature can be observed clearly in $CaTiO_3$ sample which was sintered at 900 °C showing the grains tend merges one another to form clots, this is due to inter-

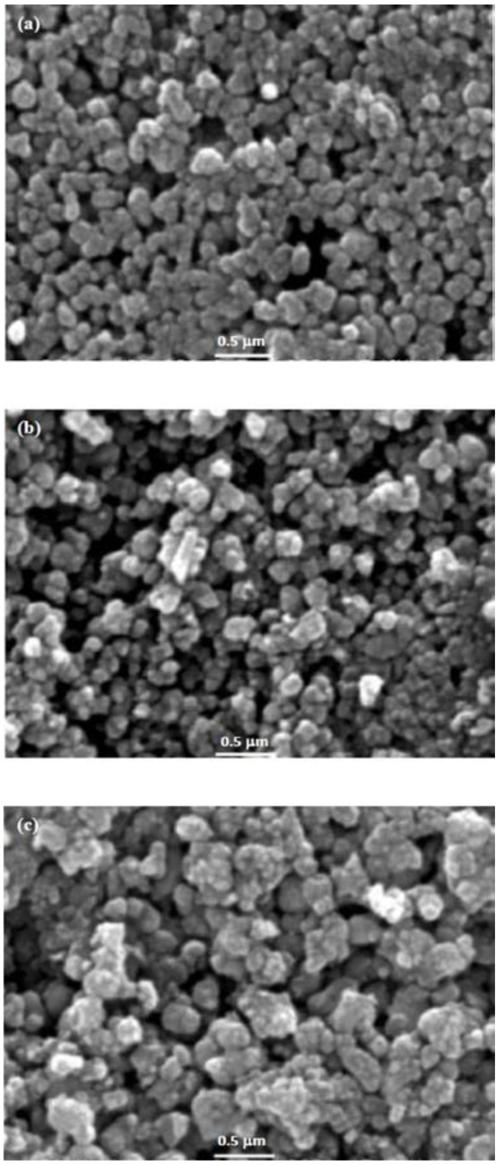

Fig. 2. Surface morphology of three TiO_3 sample for sintering at: (A) 700 °C, (B) 800 °C, (C) 900 °C.

grain diffusion has occurred due to heating at higher temperatures, as shown in Fig. 2(c). As a result of this grains diffusion were the grains to be larger and tend to be elongated.

Measurement of capacitance was carried out using LCR Meter (Hioki Hi-Tester) in a frequency range of 20 Hz-2 kHz for three samples of $CaTiO_3$ with a different sintering temperature. These measurements aimed at studying the effect of sintering temperature on the frequency response of the $CaTiO_3$ samples. Fig. 3 shows the curves of the relationship between the capacitance values with frequency for all samples with different sintering temperatures. There are no significant differences in the pattern of the curves of the three samples.

The entire sample showed high capacitance values at low frequencies (around 20 Hz), then decreased rapidly

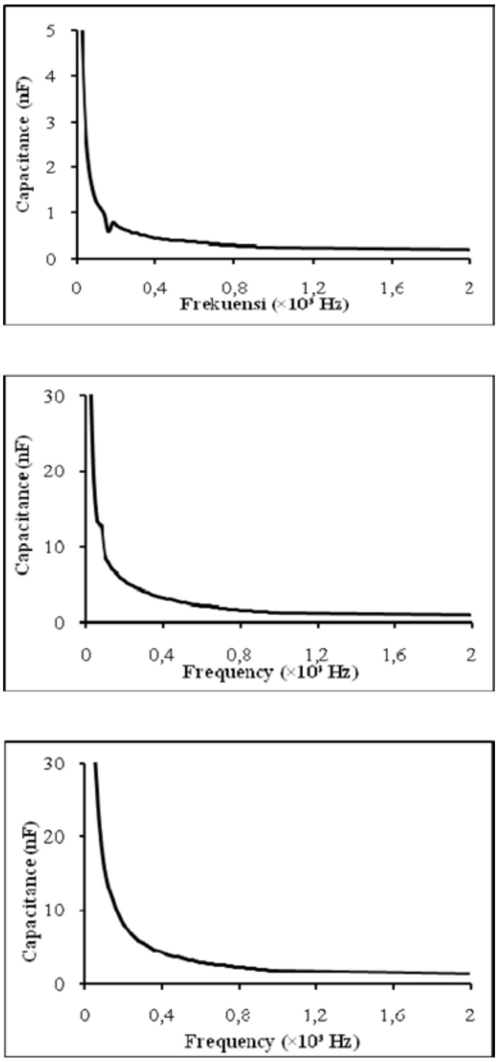

Fig. 3. Capacitance of $CaTiO_3$ sintered at (A) 700 °C, (B) 800 °C, (C) 900 °C.

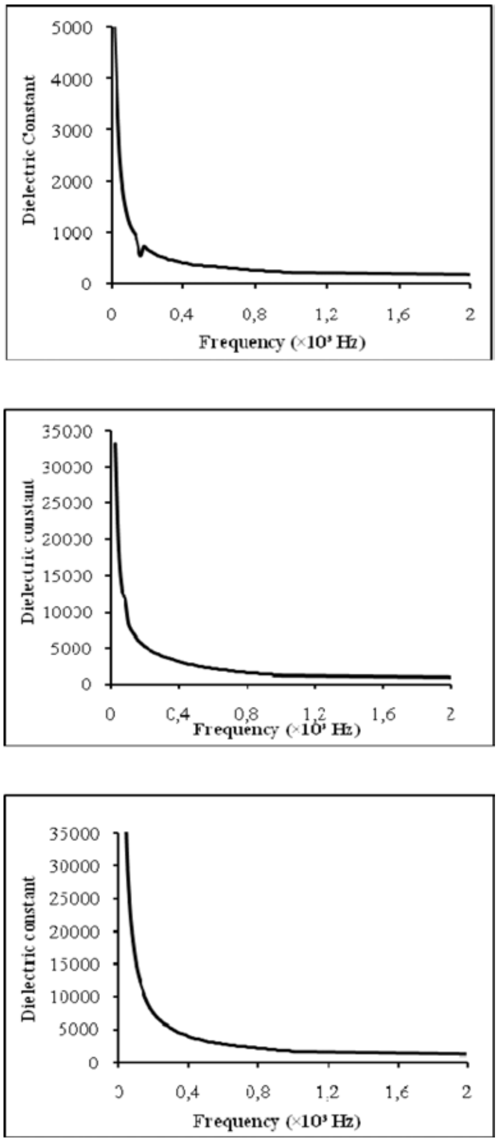

Fig. 4. Dielectric constant of $CaTiO_3$ sintered at (A) 700 °C, (B) 800 °C, and (C) 900 °C.

and curved around a frequency of 200 Hz. Further decline slowly and reach a stable at a frequency of about 800 Hz to higher frequencies. Compared to the other samples, the sample that has been sintered at 700 °C has a capacitance value is lower, ranging from low frequency to higher frequency.

The dielectric constant is an important parameter of a dielectric material, in particular for the technologies application of energy and data storage. The dielectric constant was calculated based on capacitance data obtained using LCR Meter (Hioki Hi-Tester) in the frequency range of 20 Hz-2 kHz. Fig. 4 represents the variation of the dielectric constant of $CaTiO_3$ samples that were sintered at different sintering temperatures (700 °C, 800 °C and 900 °C). At low frequencies the dielectric constant is high enough that the order of thousands to tens of thousand (´10^3-10^4) and decreased rapidly around a frequency of 200 Hz, then declined steadily to a high frequency (2 kHz).

Sample of $CaTiO_3$ sintered at a temperature of 700 °C has a dielectric constant which is much smaller than samples that were sintered at a temperature of 800 °C and 900 °C. At a frequency of 40 Hz, the value of the dielectric constant of about 2700 and has dropped to 1900 at a frequency of 60 Hz. Sample of $CaTiO_3$ that were sintered at temperature of 800 °C and 900 °C have a dielectric constant value is very high in the order of tens of thousand (´10^4) at low frequencies. For sample sintered at 800 °C, the value of the dielectric constant at a frequency of 20 Hz is around 33000 and dropped to 12700 at a frequency of 60 Hz. Likewise, the sample that was sintered at 900 °C, also have a dielectric constant value in the order of tens of thousands at low frequencies.

Differences of dielectric constant of $CaTiO_3$ sample was influenced by the crystal phases and microstructures of the sample. Sample sintered at a temperature of 700 °C was still dominated by the phase of starting materials (based on X-ray diffraction analysis), particularly TiO_2, which incidentally has a dielectric constant lower than $CaTiO_3$. With the increasing sintering temperature, the crystal phase came to be dominated by the phase of $CaTiO_3$ which increased the dielectric constant, especially for the sample which was sintered at a temperature of 900 °C. Based on the analysis of the microstructure (SEM image), it is known that the sample with the sintering temperature of 700 °C demonstrates the separated grains, consequently complicate the process of dielectric polarization in the sample. While the samples that were sintered at higher temperatures showed microstructure with grains more unified due to inter-grain diffusion so that the sample becomes more dense and solid, thus simplifying the process of charges polarization in the sample resulting in dielectric constant to be larger.

Conclusions

$CaTiO_3$ has been successfully synthesized by the hydrothermal method by utilizing the duck's eggshells as a source of calcium. The XRD results showed the dependence of sintering temperature on the crystal phase, microstructure and dielectric properties of $CaTiO_3$. The increase in the sintering temperature of the samples resulted in the $CaTiO_3$ phase increasingly dominant in the sample, on the other hand, the average crystal size (ACS) also increased with increasing sintering temperature. The SEM results showed the higher the sintering the temperature then the greater the grain size due to solid inter-grain diffusion that resulted in the unification of the granules. The measurement results of dielectric properties showed that the $CaTiO_3$ has a high dielectric constant and increasing with increased the sintering temperature.

References

1. A. Pashkin, S. Kamba, M. Berta, J. Petzelt, G.D.C. Csete de Györgyfalva, H. Zheng, H. Bagshaw and I.M. Reaney, J. Phys. D: Appl. Phys. 38 (2005) 741-748.
2. Y. Hu, Y. Zhang, H. Liu, D. Zhou, Ceramics International 37 (2011) 1609-1613.
3. M.D. Biegalski, L. Qiao, Y. Gu, A. Mehta, Q. He, Y. Takamura, A. Borisevich, and L.Q. Chen, Appl. Phys. Lett. 106 (2015) 162904.
4. J. Sedlacek, P. Ctibor, J. Kotlan and Z. Pala, Surf. Eng. 29[5] (2013) 384-389.
5. T. Bak, T. Burg, J. Nowotny, P.J. Blennerhassett, Adv. in Appl. Ceram. 106[1-2] (2007) 101-104.
6. T.M. Mazzo, G.S. do N. Libanori, M.L. Moreira, W. Avansi Jr., V.R. Mastelaro, J.A. Varela, E. Longo, J. Lumin. 165 (2015) 130-137.
7. M.L. Moreira, E.C. Paris, G.S. do Nascimento, V.M. Longo, J.R. Sambrano, V.R. Mastelaro, M.I.B. Bernardi, J. Andrés, J.A. Varela, E. Longo, Acta Mater. 57[17] (2009) 5174-5185.
8. H. Zhang, G. Chen, Y. Li, Y. Teng, Intern'l. J. Hydrogen Energy 35 (2010) 2713-2716.
9. L.M. Lozano-Sánchez, S. Obregón, L.A. Díaz-Torres, S-W Leed, V. Rodríguez-González, J. Mol. Catal. A: Chem. 410 (2015) 19-25.
10. M.R. Mohammadi and D.J. Fray, J Sol-Gel. Sci. Technol. 68 (2013) 324-333.
11. B.M. Patil, R.S. Srinivasan and S.R. Dharwadkar, Bull. Mater. Sci. 30[3] (2007) 225-229.
12. K.-H. Park and H.-G. Kim, J. Korean Phys. Soc. 56[2] (2010) 648-652.
13. S. Palaniandy and N.H. Jamil, J. Alloys and Compounds 476 (2009) 894-902.
14. X-Y. Liu, M-L. Hu, C-G. Bai, X-W. Lv, Rare Met. DOI 10.1007/s12598-014-0355-7.
15. S. Manafi, M. Jafarian, Intern'l. J. Phys. Sci. 8[23] (2013) 1277-1283.
16. T. Kimijima, K. Kanie, M. Nakaya and A. Muramatsu, Crystal Eng. Comm. 16 (2014) 5591-5597.
17. D. Wang, Z. Guo, Y. Chen, J. Hao, W. Liu, Inorg. Chem. 46 (2007) 7707-7709.
18. M. Ketta and E. Tůmová, Czech J. Anim. Sci. 61[7] (2016) 299-309.
19. T. Xian, H. Yang, Y.S. Huo, Phys. Scr. 89 (2014) 115801.
20. C. Han, J. Liu, W. Yang, Q. Wu, H. Yang, X. Xue, J Sol-Gel Sci Technol DOI 10.1007/s10971-016-4261-3.
21. M.A. Alavi, A. Morsali, J. Exper. Nanosci. 5[2] (2010) 93-105.